

Two-dimensional architectures for donor-based quantum computing

L. C. L. Hollenberg, A. D. Greentree, A. G. Fowler, and C. J. Wellard

Centre for Quantum Computer Technology, School of Physics, University of Melbourne, Parkville, VIC 3010, Australia

(Received 14 November 2005; revised manuscript received 19 April 2006; published 17 July 2006)

Through the introduction of a new electron spin transport mechanism, a 2D donor electron spin quantum computer architecture is proposed. This design addresses major technical issues in the original Kane design, including spatial oscillations in the exchange coupling strength and cross-talk in gate control. It is also expected that the introduction of nonlocality in qubit interaction will significantly improve the scaling fault-tolerant threshold over the nearest-neighbor linear array.

DOI: 10.1103/PhysRevB.74.045311

PACS number(s): 03.67.Lx

I. INTRODUCTION

The Kane paradigm of donor nuclear spin quantum computing in silicon,¹ based on single atom placement fabrication techniques,^{2,3} is an important realization of Feynman's original concept of nanotechnology in the solid state. Variations on this theme include electron spin qubits^{4–6} and charge qubits.⁷ There are significant advantages of the donor spin as a qubit, including uniformity of the confinement potential and high number of gate operations possible within the electron spin coherence time, measured to be in excess of 60 ms.⁸ Consequently, there is great interest in donor-based architectures and progress towards their fabrication.^{9–11}

It is often assumed that solid-state designs should be inherently scalable given the capabilities of semiconductor device fabrication. In reality this weak-scalability argument should be replaced with a stronger version as scalability of a given architecture is considerably more complex than fabricating many interacting qubits. Fault-tolerant scale-up requires quantum error correction over concatenated logical qubits with all the attendant ancillas, syndrome measurements, and classical feed-forward processing. Both parallelism and communication must be optimized.¹² Only by considering such systems-level issues in conjunction with the underlying qubit physics will the requirements of quantum computation in a given implementation be understood, and new concepts generated. In this paper we introduce a new mechanism for coherent donor electron spin state transport, and in a similar design path to the QCCD ion trap proposal,¹³ we construct for the first time a quasi-two-dimensional donor architecture based on distinct qubit storage and interaction regions.

The significant interest in scaling up the donor-based solid-state designs, has led to a number of works considering these scalability issues. As a result, several serious problems have been identified, including sensitivity of the exchange interaction and control to qubit placement (at the 2–3 lattice site level),^{14–16} qubit control and fabrication limitations associated with high gate densities,^{17,18} spin readout based on spin-charge transduction,^{1,19,20} and the communication bottlenecks for linear nearest neighbor (LNN) qubit arrays.^{17,21}

The issue of local versus nonlocal fault-tolerant operation is nontrivial.^{22,23} A recent surprising result is that Shor's algorithm can be implemented on a LNN circuit for the minimal qubit case with no increase at leading order in the circuit

gate count or depth.^{24,25} However, at the systems level one expects a linear nearest neighbor qubit array to suffer from swap gate overheads, particularly when concatenated qubit encoding is employed. The general analysis in Ref. 23 estimates that locality forces the threshold down inversely with the physical encoding scale. The extent of the LNN penalty has been explicitly shown to bring the threshold down by two orders of magnitude compared to the nonlocal case.²⁶

For the Kane, or related donor based architectures, all of the above implies the imperative of finding ways of traversing the linear array constraints, as the most effective way to improve the threshold and tackle the technical problems listed. An important step in this direction is the proposal for subinterfacial transport of electrons in a one-dimensional array.²⁷ This design has many desirable features, digitizing the single and two qubit gate problems in an elegant way, but also has problems with scalability due to the relative closeness of gates.¹⁷

The 2D architecture introduced here specifically addresses the problems listed above. In Fig. 1, an example of how qubit transport can be used is given for the specific case of the exchange-interaction based Kane architecture. We note that the transport ideas presented here allow for a similar, but

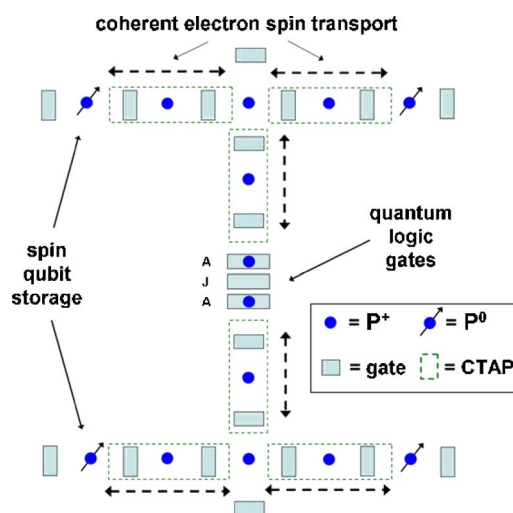


FIG. 1. (Color online) Top view of a fragment of a quasi-two-dimensional donor electron spin quantum computer architecture for the case of Si:P, incorporating coherent transport by adiabatic passage (CTAP).

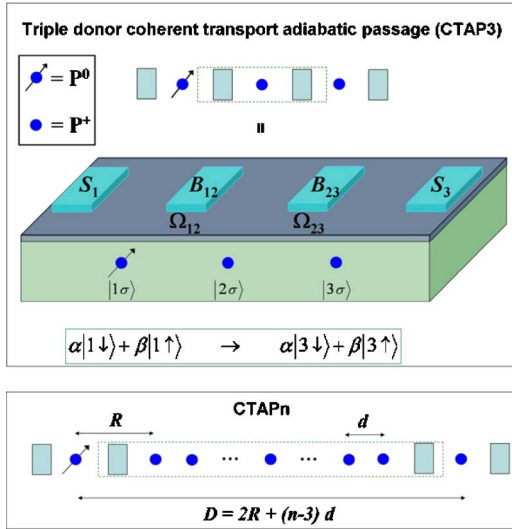


FIG. 2. (Color online) Top: Schematic of the one-electron triple donor system $3D^{2+}$ based on P donors in silicon. Two of the donors are assumed ionized, the other neutral. Bottom: multidonor CTAPn straddling schemes.

nontrivial development for the digital-Kane case. A buried array of ionized donors D^+ (which may be a spin zero species) provide pathways for coherent transport of electron spins for in-plane horizontal and vertical shuttling (dashed-border sections) of qubit states into and out of the interaction zone. The overall gate density can be further reduced by increasing the transport pathway length (Fig. 2). Initially all gates inhibit tunneling along any given channel. Coherent spin transport along one segment is achieved by adiabatically lowering the barriers in a well defined sequence to effect coherent transfer by adiabatic passage (CTAP) without populating the intervening channel donors.²⁸ We show that with appropriate donor separations, the shuttling time can be in the nanosecond range for one section. In Fig. 1 the coherent transport scheme is defined for the minimum number of donors. Higher order schemes with more donors reduces the gate density (see Fig. 2).

Logic gates are carried out in the interaction zones distinct from qubit storage regions; shown in Fig. 1 are the canonical A and J gates for electron spin based qubit control at the microsecond level.⁶ The extension of this scheme to many interaction regions is shown in Fig. 9 (below). An important point is that this design, in conjunction with newly developed characterization and calibration techniques, may be inherently defect tolerant, i.e., robust against atomic scale variations in the fabrication of the device. The recent advances in Hamiltonian identification^{29,30} demonstrate that it is possible in principle to determine the form and couplings of the two-qubit interaction to high precision using only the *in situ* architecture resources.^{31,32} After this mandatory characterization procedure, interaction regions with unacceptably low couplings can be identified and *bypassed* in the circuit flow, thereby avoiding bottleneck issues arising from the sensitivity of the exchange interaction to donor placement. This design allows for new variations on the theme, e.g., electron-nuclear singlet-triplet encoding and digitization of hyperfine

control,²⁷ or introduction of local buried B -field antennae structures,³³ and space for SET readout techniques.^{1,19,34}

II. COHERENT TRANSPORT BY ADIABATIC PASSAGE (CTAP)

A schematic of the minimal three donor transport pathway is given in Fig. 2. The triple-well system $|1\sigma\rangle$, $|2\sigma\rangle$, $|3\sigma\rangle$ ($\sigma = \uparrow, \downarrow$) facilitates coherent state transport from $\alpha|1\downarrow\rangle + \beta|1\uparrow\rangle$ to $\alpha|3\downarrow\rangle + \beta|3\uparrow\rangle$ without populating the $|2\sigma\rangle$ states. Techniques for coherent transfer by the adiabatic passage are well known,³⁵ and for the donor system was proposed in Ref. 28 for the case of charge transfer. A superconducting version of the three state case has also been proposed.³⁶ The system is controlled by shift gates, S , which can modify the energy levels of the end donors, and barrier gates, $B_{i,i+1}$ which control the tunneling rate $\Omega_{i,i+1}$ between donors i and $i+1$.

Although the scheme we introduce here necessarily includes spin, we first consider the zero field case and ignore spin degrees of freedom²⁸ to illustrate the principles of CTAP in the one-electron three-donor system, $3D^{2+}$. The effective Hamiltonian for the $3D^{2+}$ system is

$$\mathcal{H} = \Delta|2\rangle\langle 2| - \hbar(\Omega_{12}|1\rangle\langle 2| + \Omega_{23}|2\rangle\langle 3| + \text{H.c.}), \quad (1)$$

where $\Omega_{ij} = \Omega_{ij}(t)$ is the coherent tunneling rate between donors $|i\rangle$ and $|j\rangle$ and $\Delta = E_2 - E_1 = E_2 - E_3$. The eigenstates of \mathcal{H} (with energies \mathcal{E}_\pm and \mathcal{E}_0) are

$$|D_+\rangle = \sin \Theta_1 \sin \Theta_2 |1\rangle + \cos \Theta_2 |2\rangle + \cos \Theta_1 \sin \Theta_2 |3\rangle,$$

$$|D_-\rangle = \sin \Theta_1 \cos \Theta_2 |1\rangle - \sin \Theta_2 |2\rangle + \cos \Theta_1 \cos \Theta_2 |3\rangle,$$

$$|D_0\rangle = \cos \Theta_1 |1\rangle - \sin \Theta_1 |3\rangle, \quad (2)$$

where we have introduced $\Theta_1 = \arctan(\Omega_{12}/\Omega_{23})$ and $\Theta_2 = \arctan[2\hbar\sqrt{(\Omega_{12})^2 + (\Omega_{23})^2}/\Delta]/2$. Transfer from state $|1\rangle$ to $|3\rangle$ is achieved by maintaining the system in state $|D_0\rangle$ and changing the characteristics of $|D_0\rangle$ adiabatically ($|\mathcal{E}_0 - \mathcal{E}_\pm| \gg \langle D_0 | \mathcal{D}_\pm \rangle$) from $|1\rangle$ at $t=0$ to $|3\rangle$ at $t=t_{\max}$ by appropriate control of the tunneling rates, without population leakage into the other eigenstates.

For the case of coherent spin transport we write the $3D^{2+}$ Hamiltonian in terms of spin/site operators as

$$\mathcal{H} = \sum_{i=1}^3 \sum_{\sigma=\uparrow,\downarrow} E_{i\sigma} c_{i\sigma}^\dagger c_{i\sigma} + \sum_{(ij)} \sum_{\sigma=\uparrow,\downarrow} \Omega_{ij}(t) c_{j\sigma}^\dagger c_{i\sigma}. \quad (3)$$

The system defined in Eq. (3) is solved numerically for the density matrix, $\rho(t)$, in the presence of a (dominant) charge dephasing rate Γ , assumed to act equally on all coherences. Calculations (discussed below) indicate that spin and charge degrees of freedom are essentially decoupled in this system, hence we are able to neglect spin-orbit and hyperfine terms to leading order. Without attempting to fully optimize control we apply Gaussian pulses of the form

$$\Omega_{ij}(t) = \Omega_{ij}^{\max} \exp[-(t - t_{ij})^2 / (2w_{ij}^2)], \quad (4)$$

where t_{ij} and w_{ij} are the peak time and width of the control pulse modulating the tunneling rate between position states

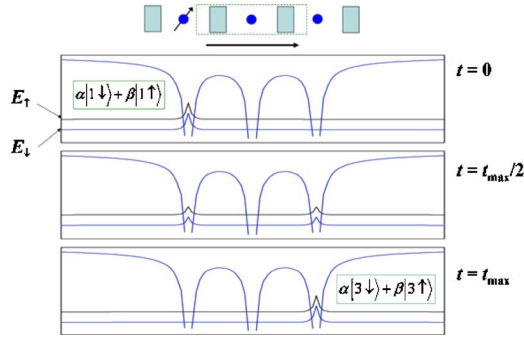


FIG. 3. (Color online) Numerical simulation of the CTAP pulse scheme applied to a spin superposition at donor 1 at $t=0$, demonstrating coherent transfer to the third donor at $t=t_{\max}$ (phases relative to an untransported state).

$|i\rangle$ and $|j\rangle$. To simplify matters for initial simulations we set the maximum tunneling rates and standard deviations for each transition to be equal, i.e., $\Omega_{ij}^{\max} = \Omega^{\max}$ and $w_{ij} = w$, and set $\Delta = 0$ (these conditions can be relaxed with no effect on the conclusions of this paper). Transfer is then optimized when the width of the pulses equals the time delay between the pulses.³⁷ With total pulse time t_{\max} , we choose $w = t_{\max}/8$ so that $t_{12} = (t_{\max} + w)/2$ and $t_{23} = (t_{\max} - w)/2$. This ordering, where Ω_{23} is applied *before* Ω_{12} is known as the counterintuitive pulse sequence and has significant advantages in improving transfer fidelity over other pulse sequences.²⁸ The results of such calculations are given in Fig. 3, where the initial state at site 1 was taken to be a spin superposition state $\alpha|1\downarrow\rangle + \beta|1\uparrow\rangle$ (we set $\alpha = \beta = 1/\sqrt{2}$ in this specific case without loss of generality). The qubit is transported to the required state $\alpha|3\downarrow\rangle + \beta|3\uparrow\rangle$ at site 3 at $t = t_{\max}$. Since we have used the counterintuitive pulse ordering, at no time during the sequence does the electron occupy the middle site.

In a real system, transport fidelity will be controlled by the adiabatic criterion and the time scale of any charge dephasing, with respect to the controlled interdonor tunneling rates. In solving the time dependence of the open system in the presence of charge dephasing for a range of parameter values, we find quite generally that the fidelity is high when the adiabaticity criterion is satisfied, and the transport time is at least an order of magnitude faster than charge dephasing. These results are consistent with those of Ivanov *et al.*³⁸ who considered the role of dephasing in the three-state stimulated

Raman adiabatic passage (STIRAP). The requirements on coherence for transport are much less stringent than for a charge based qubit system, as we require coherence only over a single transport cycle. Although these competing time scales are essentially unmeasured at present, estimates for the P-P⁺ decoherence time are of order 10 ns (Ref. 40) or longer,³⁹ and a value of 220 ns was reported recently for a Si:P double dot.⁴¹ On the other hand, transport time scales are dominated by subnanosecond tunneling times, due to the strong confining potential of donor nuclei. In order to quantitatively determine the effect of such time scales on transport fidelity, we must first determine the typical interdonor tunneling times through a detailed analysis of the gated P-P⁺ system.

III. GATE ASSISTED TUNNELING BETWEEN DONORS

The CTAP transport time will be defined primarily by the gate-assisted tunneling rate between donors. While recent investigations of the P-P⁺ system in a uniform electric field have been reported for a uniform dc field⁴² and the full driven ac case,⁴³ we require here the interdonor barrier response to the field generated by a surface gate. Our approach is to use the TCAD nanoelectronic design package to compute the potential $V(\mathbf{r})$ due to a surface B -gate bias V_b (Fig. 4) and numerically calculate the P-P⁺ molecular donor electron wave function for the first two states in this external potential, and hence determine the effective tunneling rate.

We choose an effective mass basis, e.g., $F_{\pm z}^{n,l,m}(\mathbf{r}) = \varphi_{n,l,m}(x, y, \gamma z)$, about the six band minima where the $\varphi_{n,l,m}$ are hydrogenic orbitals with Bohr radius a_{\perp} , and $\gamma = a_{\perp}/a_{\parallel}$. Diagonalizing the total Hamiltonian of the system, we obtain a generalized Kohn-Luttinger wave function,

$$\psi(\mathbf{r}, V_b) = \sum_{n=1}^{n_{\max}} \sum_{l,m} c_{n,l,m}(V_b) \sum_{\mu=1}^6 F_{\mu}^{n,l,m}(\mathbf{r}) e^{i\mathbf{k}_{\mu} \cdot \mathbf{r}} u_{\mathbf{k}_{\mu}}(\mathbf{r}), \quad (5)$$

where the Bloch states are

$$u_{\mathbf{k}_{\mu}}(\mathbf{r}) = \sum_{\mathbf{G}} A_{\mathbf{k}_{\mu}}(\mathbf{G}) e^{i\mathbf{G} \cdot \mathbf{k}_{\mu}}. \quad (6)$$

The silicon band structure is incorporated via the $A_{\mathbf{k}_{\mu}}(\mathbf{G})$, which are computed using the pseudopotentials method.⁴⁴ To describe the extended P-P⁺ system we form bonding and antibonding states

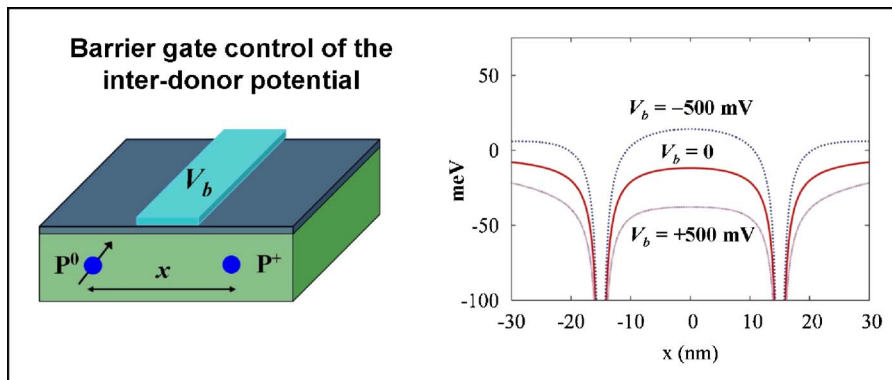


FIG. 4. (Color online) Response of the P-P⁺ interdonor potential profile to the barrier gate bias $V_b = (0, \pm 500)$ mV.

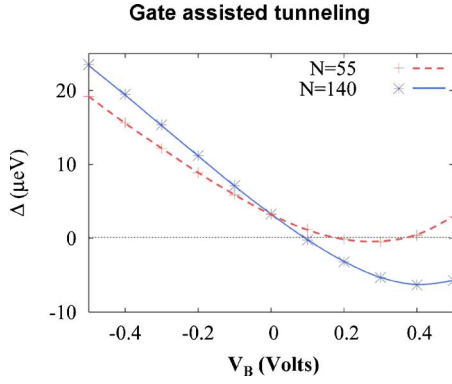


FIG. 5. (Color online) Computed energy gap for the P-P⁺ system as a function of *B*-gate bias V_b for $R=30$ nm and basis sizes $N=55$ and 140 (device parameters are: 30 nm donor depth below the oxide interface, 5 nm oxide thickness, and 10 nm gate width).

$$\Psi_{\pm}(\mathbf{r}, V_b) = \mathcal{N}(\psi_L(\mathbf{r}, V_b) \pm \psi_R(\mathbf{r}, V_b)), \quad (7)$$

normalized by \mathcal{N} , and compute the gate bias dependent gap $\Delta(V_b)$ as shown in Fig. 5 for basis sizes 55 and 140 ($n_{\max} = 5$ and 7, respectively). Comparison of the linear regions indicates that the range of validity is approximately $|V_b| \lesssim 200$ mV. These are the first calculations including band-structure details to probe the effect of a gate bias on the interdonor barrier and resultant quantum control of a single donor electron in a buried donor molecular structure. Beyond the effective mass approximation, larger scale computations using either the new band-basis expansion formalism⁴⁵ or optimized tight-binding⁴⁶ would be required to verify the barrier control range determined here.

In contrast to what one expects for an isolated P-P⁺ system in vacuum where the nodal structure of the bonding and

antibonding states is simple, the nontrivial nodal properties of the donor electron wave function and the proximity of the oxide interface complicates the tunneling control. These calculations directly extend similar effects noted in the ungated P-P⁺ system.⁴⁷ From Fig. 5 we see that for this configuration the tunneling rate can be varied from 0 at +100 mV to ~ 10 GHz at -200 mV, giving a gate assisted tunneling time of 60 ps.

IV. ADIABATICITY AND FIDELITY IN THE CTAP TRANSPORT SCHEME

Based on the gate assisted tunneling times determined in the previous section, we carried out time-dependent simulations of the CTAP protocol for 5, 7, and 9 donor chains. First, however, we show analytical results to highlight the general scaling relations. To investigate the fidelity of transfer as the number of donors in the chain is varied, we must satisfy the adiabaticity criteria. As with the three-donor case, the states of interest are those closest to the generalization of $|\mathcal{D}_0\rangle$, which we denote as $|\mathcal{D}_{\pm,n}\rangle$. The eigenvalues for $|\mathcal{D}_{\pm,n}\rangle$ are approximately

$$\Lambda_{\pm}(n) = \pm \sqrt{\frac{2(\Omega_1^2 + \Omega_2^2)}{n-1}}. \quad (8)$$

Explicitly, the states are given by ($n=2m+1$),

$$|\mathcal{D}_{0,n}\rangle = \frac{\Omega_{n-1,n}|1\rangle + (-1)^m \Omega_1|n\rangle + \sum_{k=1}^{m-1} (-1)^k \frac{\Omega_1 \Omega_2}{\Omega_s} |2k+1\rangle}{\sqrt{\Omega_1^2 + \Omega_2^2}}, \quad (9)$$

$$|\mathcal{D}_{\pm,n}\rangle = \frac{\Omega_1|1\rangle - (-1)^m \Omega_2|n\rangle + \Lambda_{\pm}(n)|2\rangle + \sum_{k=2}^m A_k(n)|2k-1\rangle - (-1)^k \Lambda_{\pm}(n)|2k\rangle}{\sqrt{2}\sqrt{\Omega_1^2 + \Omega_2^2}}, \quad (10)$$

where $A_k(n) = (-1)^k \left[\frac{(k-1)\Lambda_{\pm}(n)^2 - \Omega_1^2}{\Omega_s} \right]$, and we have assumed $\Omega_s \gg \Omega_1, \Omega_2$ and dropped terms in $(1/\Omega_s)^2$ and higher. For high-fidelity transfer we require the system to remain in the equivalent of state $|\mathcal{D}_0\rangle$, without making a nonadiabatic transfer to one of the neighboring states, i.e., $|\mathcal{D}_{\pm}\rangle$. As a rule of thumb this means that the time for the protocol must be short compared to $1/\Lambda_{\pm}(n)$. More precisely, we must satisfy

$$A = \frac{\langle \beta | \frac{\partial \mathcal{H}}{\partial t} | \alpha \rangle}{|\langle \beta | \mathcal{H} | \beta \rangle - \langle \alpha | \mathcal{H} | \alpha \rangle|} \ll 1 \quad (11)$$

for two neighboring transitions, $|\alpha\rangle$ and $|\beta\rangle$. The transitions of interest are those between $|\mathcal{D}_{0,n}\rangle$ and $|\mathcal{D}_{+,n}\rangle$, and $|\mathcal{D}_{0,n}\rangle$ and

$|\mathcal{D}_{-,n}\rangle$, which will be equivalent for the purposes of adiabaticity, so for simplicity, we choose the former. In this case, the adiabaticity parameter can be derived analytically and is

$$A = \frac{1}{\sqrt{2}(\Omega_1^2 + \Omega_2^2)} \left[\sqrt{\frac{n-1}{2(\Omega_1^2 + \Omega_2^2)}} (\dot{\Omega}_1 \Omega_2 - \dot{\Omega}_2 \Omega_1) + \frac{\Omega_1 \Omega_2 n}{\Omega_s (\Omega_1^2 + \Omega_2^2)} (\dot{\Omega}_2 \Omega_2 - \dot{\Omega}_1 \Omega_1) \right]. \quad (12)$$

This should be compared to the result for adiabaticity in the STIRAP scheme,³⁵ where the first term is the usual result scaled by the increase in states, and the second term is a higher order correction.

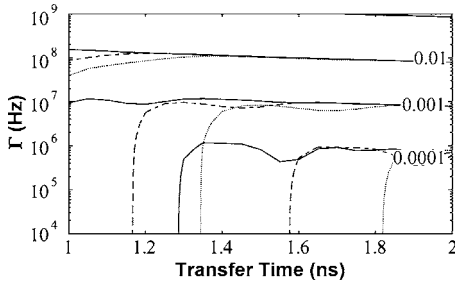


FIG. 6. Transfer error (contours) as a function of charge dephasing rate, Γ and total transfer time for CTAP5 (solid line), CTAP7 (long dashes), and CTAP9 (short dashes) for the case of 30 nm end-donor spacings, and 20 nm between the central donors ($\Omega_{\text{end}}^{\text{max}} = 87$ GHz and $\Omega_S = 1$ THz).

The analysis for adiabaticity is useful for estimating ranges and pulse times, but to calculate the actual transfer fidelities it is necessary to numerically evolve the open system through the adiabatic transfer. In terms of the population $\rho_{nn}(t)$ at the end site, n , the transport error ϵ_n for the CTAPn protocol over a t_{max} is defined as $\epsilon_n = 1 - \rho_{nn}(t_{\text{max}})$. We have solved the system, including the effect of dephasing and the results are shown in Fig. 6. The adiabatic nature of the transport scheme provides an inherent robustness, as evidenced in Fig. 6, which shows a remarkable uniformity in the response to charge dephasing for the different path lengths once the adiabatic regime is reached. The extent to which Γ controls the transport fidelity is also clear, and we note that there is room for improvement through optimization of control pulses and minimization of charge fluctuations through fabrication development.

As intrinsic spin-orbit coupling for donor states in silicon is very low, dephasing of donor electron spin is dominated

by spectral diffusion due to spin impurities and is mitigated by isotopic purification.⁴⁸ For the bound state spin-orbit coupling, at $V_b \sim 200$ mV we calculate from Eq. (5) the non- S components to be $\sum_{n,l>0,m} |c_{n,l,m}(V_b)|^2 < 10^{-4}$ indicating that the deviation from the S sector is minimal. Together with near zero occupation of channel states, this suggests that charge dephasing will have a negligible second order effect on the spin coherence during transport. Decoupling of orbital and spin sectors has already given rise to demonstrations of coherent transport of electron spins over 100 μm in GaAs.⁴⁹

This first order decoupling of charge and spin sectors also occurs for the hyperfine interactions of the electron spin with channel donors. Even in the presence of charge dephasing the degree of channel population is very low, and this fact combined with the relatively fast time scale of transport (nanoseconds) compared to the hyperfine interaction (microseconds) will lead to an extremely low higher order error. We verified this numerically by including hyperfine interactions during the CTAP protocol, over an ensemble of channel donor nuclear spin configurations and found the contribution to overall transport error was negligible.

Another important consequence of adiabaticity is that relatively large variations in tunneling rates due to donor placement⁴⁷ will not affect the viability of the scheme. The results of explicit calculations for tunneling rate variations (as defined in Fig. 7) presented in Fig. 8 show that relatively large variations can be tolerated.

V. ARCHITECTURES FOR FAULT-TOLERANT OPERATION

The basic layout of a possible quasi-two-dimensional architecture, with interacting qubit pairs, storage regions,

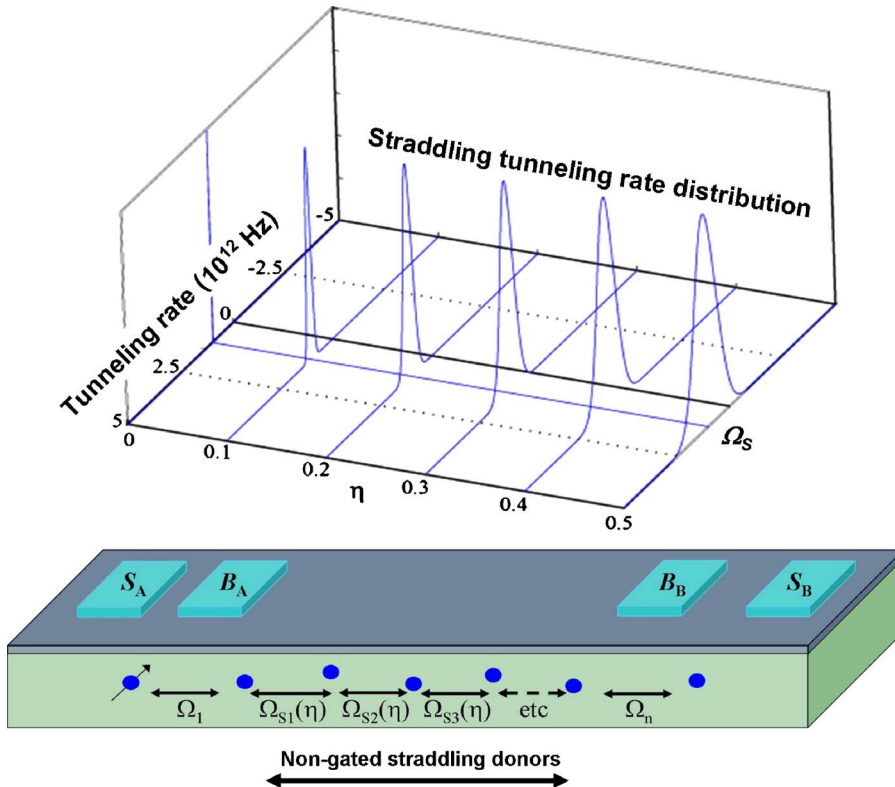


FIG. 7. (Color online) Distribution of nonuniform interdonor tunneling rates arising from fabrication variations in donor placement, where the Ω_{S_i} are chosen randomly from a normal distribution with mean Ω_S and standard deviation $\eta\Omega_S$.

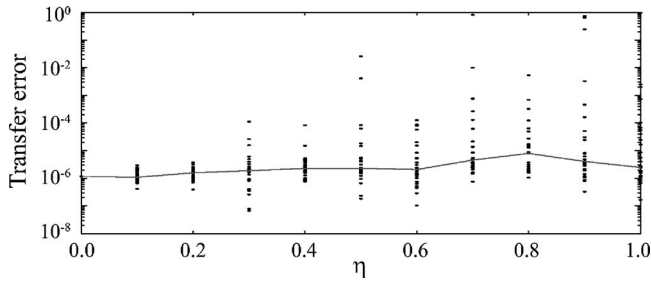


FIG. 8. Error rates due to misalignment of the central donors as a function of the distribution parameter η which governs the standard deviation around the target straddling donor tunneling rate $\Omega_S=1$ THz ($t_{\max}=2$ ns). The line is the median error rate, over the ensemble for each η .

transport pathways based on CTAP9, and classical driving circuitry is shown in Fig. 9. The overall effective linear gate density still is comparable to the original Kane proposal, but it has the significant advantages of greatly reduced crosstalk between interacting pairs of qubits, the ability to bypass interaction regions with an insufficiently strong exchange in-

teraction, the ability to quickly transport qubits large distances allowing the effective implementation of nonlocal gates, and the physical incorporation of the relatively large SET readout devices which was absent in the original design. The placement of SET sites may ultimately be important in providing a heralding mechanism for correctable transport errors. Linear gate density could be further reduced by using longer CTAP transport rails, and possibly by replacing each A-gate and S-gate pair at the interaction regions with a single offset gate and globally controlling every second S-gate in the transport/storage regions instead of each one individually.

One would expect that the optimum arrangement for fault-tolerant operation may require sophisticated system level simulations comparable to those described in Ref. 50 to determine the best use of this medium range quantum transport capability, and the resulting effective threshold.

VI. CONCLUSIONS

In this paper we have presented a 2D donor quantum computer architecture proposal based on nonballistic spin transport. For definiteness, our chosen context is an electron

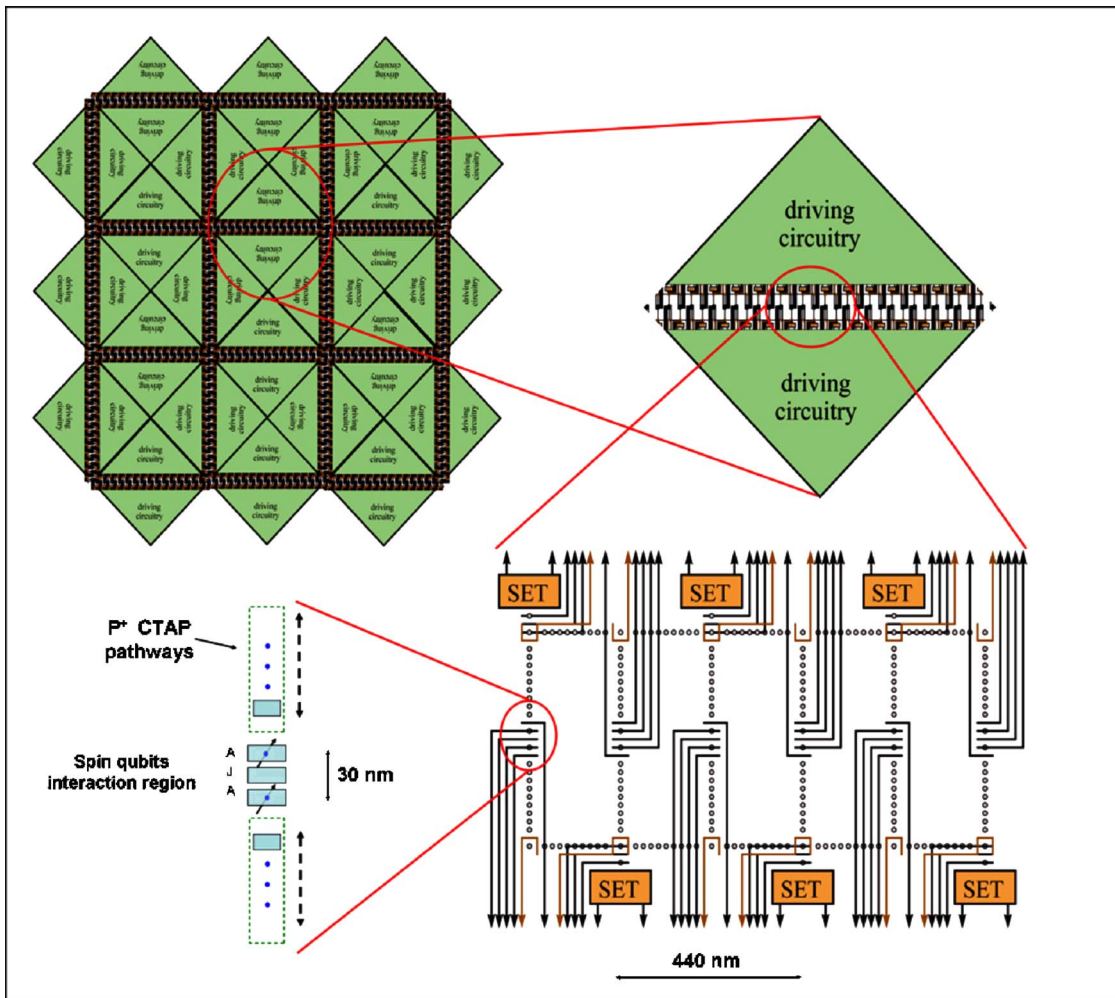


FIG. 9. (Color online) The figure shows (counterclockwise from the bottom left) the CTAP rails connecting the interaction regions with the rest of the computer; the incorporation of interaction zones, storage, and SET readout; a unit cell including space reserved for classical driving circuitry on a chip; and a quasi-two-dimensional tiled arrangement which can be extended in the plane.

spin qubit encoding with hyperfine and exchange gates, however, we note that there are a number of other potentially useful donor-based qubit schemes to explore. It is clear that the introduction of coherent spin transport to donor quantum computing allows us to address many problems in the Kane concept, and consider scalable fault-tolerant architectures with low gate densities, room for SET structures and control, and importantly a bypass mechanism for low value exchange gates. One expects the realities of the silicon crystalline environment will necessitate the characterization of transport pathways, however, the precision requirements of the adiabatic CTAP mechanism would be far less than the quantum gate threshold. Importantly, the designs proposed here provide, in conjunction with *in situ* characterization protocols, a path towards atomic level defect-tolerant donor architectures.

Note added in proof: Following initial submission of this work, two related papers came to our attention. In the first, a

2D architecture for GaAs systems has been proposed, which should share some of the same advantages of the present scheme.⁵¹ In the second, Svore *et al.*⁵² explicitly consider the effect of including transport and optimal arrangements in a 2D lattice on the fault-tolerant threshold. This important general analysis of the 2D lattice with swap gate transport may carry directly over to our case with swap gates and “dummy” qubits replaced by CTAP transport rails and vacant sites.

ACKNOWLEDGMENTS

This work was supported by the Australian Research Council, the Australian Government, and the U.S. National Security Agency (NSA), Advanced Research and Development Activity (ARDA), and the Army Research Office (ARO) under Contract No. W911NF-04-1-0290.

-
- ¹B. E. Kane, *Nature (London)* **393**, 133 (1998).
²S. R. Schofield, N. J. Curson, M. Y. Simmons, F. J. Rueß, T. Hallam, L. Oberbeck, and R. G. Clark, *Phys. Rev. Lett.* **91**, 136104 (2003).
³D. N. Jamieson, C. Yang, T. Hopf, S. M. Hearne, C. I. Pakes, S. Prawer, M. Mitic, E. Gauja, S. E. Andresen, F. E. Hudson, A. S. Dzurak, and R. G. Clark, *Appl. Phys. Lett.* **86**, 202101 (2005).
⁴R. Vrijen, E. Yablonovitch, K. Wang, H. W. Jiang, A. Balandin, V. Roychowdhury, T. Mor, and D. DiVincenzo, *Phys. Rev. A* **62**, 012306 (2000).
⁵R. de Sousa, J. D. Delgado, and S. Das Sarma, *Phys. Rev. A* **70**, 052304 (2004).
⁶C. D. Hill, L. C. L. Hollenberg, A. G. Fowler, C. J. Wellard, A. D. Greentree, and H.-S. Goan, *Phys. Rev. B* **72**, 045350 (2005).
⁷L. C. L. Hollenberg, A. S. Dzurak, C. Wellard, A. R. Hamilton, D. J. Reilly, G. J. Milburn, and R. G. Clark, *Phys. Rev. B* **69**, 113301 (2004).
⁸A. M. Tyryshkin, S. A. Lyon, A. V. Astashkin, and A. M. Raitsimring, *Phys. Rev. B* **68**, 193207 (2003).
⁹R. G. Clark, R. Brenner, T. M. Buehler, V. Chan, N. J. Curson, A. S. Dzurak, E. Gauja, H. S. Goan, A. D. Greentree, T. Hallam, A. R. Hamilton, L. C. L. Hollenberg, D. N. Jamieson, J. C. McCallum, G. J. Milburn, J. L. O’Brien, L. Oberbeck, C. I. Pakes, S. D. Prawer, D. J. Reilly, F. J. Ruess, S. R. Schofield, M. Y. Simmons, F. E. Stanley, R. P. Starrett, C. Wellard, and C. Yang, *Philos. Trans. R. Soc. London, Ser. A* **361**, 1451 (2003).
¹⁰T. Schenkel, A. Persaud, S. J. Park, J. Nilsson, J. Bokor, J. A. Liddle, R. Keller, D. H. Schneider, D. W. Cheng, and D. E. Humphries, *J. Appl. Phys.* **94**, 7017 (2003).
¹¹T. M. Buehler, V. Chan, A. J. Ferguson, A. S. Dzurak, F. E. Hudson, D. J. Reilly, A. R. Hamilton, R. G. Clark, D. N. Jamieson, C. Yang, C. I. Pakes, and S. Prawer, *Appl. Phys. Lett.* **88**, 192101 (2006).
¹²A. Steane, in *Decoherence and its Implications in Quantum Computation and Information Transfer*, edited by A. Gonis and P. E. A. Turchi (IOS, Amsterdam, 2001), pp. 284–298.
¹³D. Kielpinksy, C. Monroe, and D. J. Wineland, *Nature (London)* **417**, 709 (2002).
¹⁴B. Koiller, X. Hu, and S. Das Sarma, *Phys. Rev. Lett.* **88**, 027903 (2002).
¹⁵C. J. Wellard, L. C. L. Hollenberg, F. Parisoli, L. Kettle, H.-S. Goan, J. A. L. McIntosh, and D. N. Jamieson, *Phys. Rev. B* **68**, 195209 (2003).
¹⁶B. E. Kane, *MRS Bull.* **30**, 105 (2005).
¹⁷M. Oskin, F. T. Chong, I. Chuang, and J. Kubiatowicz, in *Building Quantum Wires: The Long and the Short of It*, Proceedings of the 30th Annual International Symposium on Computer Architecture (ISCA), San Diego, June 2003.
¹⁸D. Copley, M. Oskin, F. Impens, T. Metodiev, A. Cross, F. T. Chong, I. L. Chuang, and J. Kubiatowicz, *IEEE J. Sel. Top. Quantum Electron.* **9** (6), 1552 (2003).
¹⁹L. C. L. Hollenberg, C. J. Wellard, C. I. Pakes, and A. G. Fowler, *Phys. Rev. B* **69**, 233301 (2004).
²⁰M. J. Testolin, Andrew D. Greentree, C. J. Wellard, and L. C. L. Hollenberg, *Phys. Rev. B* **72**, 195325 (2005).
²¹T. Metodiev, D. Copley, F. T. Chong, I. Chuang, M. Oskin, and J. Kubiatowicz, in *A Brief Comparison: Ion-Trap and Silicon-Based Implementations of Quantum Computation*, Proceedings of the 2nd Workshop on Non-Silicon Computing (NSC) held in conjunction with the 30th Annual International Symposium on Computer Architecture (ISCA), San Diego, June 2003.
²²D. Gottesman, *J. Mod. Opt.* **47**, 333 (2000).
²³K. M. Svore, B. M. Terhal, and D. P. DiVincenzo, *Phys. Rev. A* **72**, 022317 (2005).
²⁴A. Fowler, S. Devitt, and L. Hollenberg, *Quantum Inf. Comput.* **4**, 237 (2004).
²⁵S. J. Devitt, A. G. Fowler, and L. C. L. Hollenberg, *quant-ph/0408081*, *Quantum Inf. Comput.* (to be published).
²⁶T. Szkopek, P. O. Boykin, H. Fan, V. P. Roychowdhury, E. Yablonovitch, G. Simms, M. Gyure, and B. Fong, *IEEE Trans. Nanotechnol.* **5**, 42 (2006).
²⁷A. J. Skinner, M. E. Davenport, and B. E. Kane, *Phys. Rev. Lett.* **90**, 087901 (2003).
²⁸A. D. Greentree, J. H. Cole, A. R. Hamilton, and L. C. L. Hollenberg, *Phys. Rev. B* **70**, 235317 (2004).
²⁹S. G. Schirmer, A. Kolli, and D. K. L. Oi, *Phys. Rev. A* **69**,

- 050306(R) (2004).
- ³⁰J. H. Cole, S. G. Schirmer, A. D. Greentree, C. J. Wellard, D. K. L. Oi, and L. C. L. Hollenberg, *Phys. Rev. A* **71**, 062312 (2005).
- ³¹J. H. Cole, S. J. Devitt, and L. C. L. Hollenberg, quant-ph/0508229 (unpublished).
- ³²Simon J. Devitt, Jared H. Cole, and Lloyd C. L. Hollenberg, *Phys. Rev. A* **73**, 052317 (2006).
- ³³D. A. Lidar and J. H. Thywissen, *J. Appl. Phys.* **96**, 754 (2004).
- ³⁴A. D. Greentree, A. R. Hamilton, L. C. L. Hollenberg, and R. G. Clark, *Phys. Rev. B* **71**, 113310 (2005).
- ³⁵N. V. Vitanov, T. Halfmann, B. W. Shore, and K. Bergmann, *Annu. Rev. Phys. Chem.* **52**, 763 (2001).
- ³⁶J. Siewert and T. Brandes, *Adv. Solid State Phys.* **44**, 181 (2004).
- ³⁷U. Gaubatz, P. Rudecki, S. Schiemann, and K. Bergmann, *J. Chem. Phys.* **92**, 5363 (1990).
- ³⁸P. A. Ivanov, N. V. Vitanov, and K. Bergmann, *Phys. Rev. A* **70**, 063409 (2004).
- ³⁹S. D. Barrett and G. J. Milburn, *Phys. Rev. B* **68**, 155307 (2003).
- ⁴⁰L. Fedichkin and A. Fedorov, *Phys. Rev. A* **69**, 032311 (2004).
- ⁴¹J. Gorman, E. G. Emiroglu, D. G. Hasko, and D. A. Williams, *Phys. Rev. Lett.* **95**, 090502 (2005).
- ⁴²B. Koiller, X. Hu, and S. Das Sarma, *Phys. Rev. B* **73**, 045319 (2006).
- ⁴³C. J. Wellard, L. C. L. Hollenberg, and S. Das Sarma, cond-mat/0512107, *Phys. Rev. B* (to be published).
- ⁴⁴For details see, L. C. L. Hollenberg, C. J. Wellard, and A. D. Greentree, *Handbook of Theoretical and Computational Nanotechnology*, edited by M. Rieth and W. Schommers (ASP Publishers, Stevensons Ranch, 2006).
- ⁴⁵C. J. Wellard and L. C. L. Hollenberg, *Phys. Rev. B* **72**, 085202 (2005).
- ⁴⁶A. S. Martins, T. B. Boykin, G. Klimeck, and B. Koiller, *Phys. Rev. B* **72**, 193204 (2005).
- ⁴⁷X. Hu, B. Koiller, and S. Das Sarma, *Phys. Rev. B* **71**, 235332 (2005).
- ⁴⁸R. de Sousa and S. Das Sarma, *Phys. Rev. B* **68**, 115322 (2003).
- ⁴⁹J. M. Kikkawa and D. D. Awschalom, *Nature (London)* **397**, 139 (1999).
- ⁵⁰D. Copley, M. Oskin, A. Cross, T. Metodiev, F. T. Chong, I. Chuang, and J. Kubiawicz, *30th International Symposium on Computer Architecture*, Illinois, 2003.
- ⁵¹J. M. Taylor, H.-A. Engel, W. Dur, A. Yacoby, C. M. Marcus, P. Zoller, and M. D. Lukin, *Nat. Phys.* **1**, 177 (2005).
- ⁵²K. M. Svore, D. P. DiVincenzo, and B. M. Terhal, quant-ph/0604090 (unpublished).